Entrainer selection using the Infinitely Sharp Split method and thermodynamic criteria for separating binary minimum-boiling azeotrope by extractive distillation

Ivonne Rodriguez-Donis, Edoardo Parascandolo, Jens Abildskov, Vincent Gerbaud, Nataliya Shcherbakova

Entrainer selection using the Infinitely Sharp Split method and thermodynamic criteria for separating binary minimum-boiling azeotrope by extractive distillation

Ivonne Rodriguez-Donis[1]*, Nataliya Shcherbakova[2], Edoardo Parascandolo[3], Jens Abildskov[4], Vincent Gerbaud[2]

[1] Laboratoire de Chimie Agro-industrielle, LCA, Université de Toulouse, INRA, Toulouse, France
[2] Laboratoire de Génie Chimique, Université de Toulouse, CNRS, INP, UPS Toulouse, France
[3] Dipartimento di Chimica, Materiali e Ingegneria Chimica, Politecnico di Milano, Italy
[4] PROSYS, Department of Chemical and Biochemical Engineering, Building 228A, Technical University of Denmark, 2800 Kgs. Lyngby, Denmark

*Corresponding author e-mail address: vincent.gerbaud@ensiacet.fr

ABSTRACT

Entrainer selection for extractive distillation remains a challenge because established criteria are based on thermodynamic properties at entrainer infinite dilution, primarily developed for an extractive column. However, a cost-effective extractive distillation continuous process uses two connected - extractive and entrainer regeneration - distillation columns. Using only the ternary mixture A-B-E vapor-liquid equilibrium data, the Infinitely Sharp Split (ISS) method is combined with the driving force concept as a new thermodynamic criterion, to compare the performance of entrainers for extractive distillation process. The ISS method allows fast computation of the minimum value of both the entrainer flowrate and the reflux ratio for the extractive distillation column, while the driving force concept is related to the regeneration column design. The methodology is applied to the separation of the minimum-boiling azeotrope methanol – dimethyl carbonate with a list of five high boiling entrainers, giving methanol as distillation product of the extractive distillation column. The entrainer ranking proposed by the combined criterion agrees with optimization results of the two-column extractive distillation process. The best candidate, methyl salicylate, having the lowest minimum entrainer flow rate and reflux ratio, provides also the most cost-effective extractive distillation process.

Keywords: extractive distillation, entrainer selection, Infinitely Sharp Split, driving force, isovolatility curves

1. Introduction

Extractive distillation is a well-established method of separation of binary azeotropic pairs (A+B) in chemical and pharmaceutical industries. The method requires addition of a so-called entrainer, E. The entrainer interacts preferentially with one component of the mixture forming the azeotrope. However, formation of additional azeotropic pairs, between the entrainer E and the compounds A and B, must be avoided. Indeed, the primary condition for choosing an entrainer is feasibility. The resulting residue curve map must match one of the well-established feasible extractive separation types described by Serafimov's ternary diagram classes 1.0-1a, 1.0-1b, 1.0-2 or 0.0-1. However, other factors must be considered such as energy consumption and CAPEX (capital expenditures), with direct impact on the total cost of the extractive distillation process. Besides, an environmentally friendly bio-based entrainer is preferably based on the assessment of substance-specific hazards with the quantification of emissions and resource use over its full life-cycle.

The simplest and most common extractive distillation flowsheet in continuous mode has two connected distillation columns (Fig. 1) for separating a minimum-boiling azeotropic mixture A-B with an entrainer E having the maximum-boiling temperature in the resulting ternary mixture. The flowsheet corresponds to the separation of a ternary mixture belonging to 1.0-1a Serafimov class (Kiva et al., 2003)

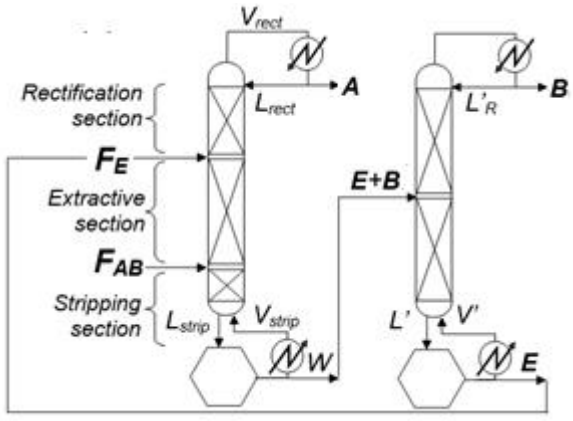

Fig. 1. Typical configuration of the extractive distillation process for separating a minimum -boiling azeotropic mixture A-B with a high boiler entrainer E (Gerbaud et al., 2019, with permission from Elsevier)

The entrainer is fed, with flowrate F_E, into the first extractive distillation column (left column) between the main feed tray (F_{AB}) and the column top providing an extractive section where separation of A and B takes place under a constant entrainer concentration. The second column (right column) is used to regenerate the entrainer, to be recycled to the first column. If the addition of the entrainer increases the relative volatility of compound A, then A is the distillate product. The binary mixture B+E then forms the extractive column bottoms product, and is fed

to the second distillation column, where B is the distillate and the entrainer is the bottom product, to be recycled. The choice of the entrainer is crucial for the process feasibility (Lei et al., 2003, Gerbaud et al. 2019) as it stipulates the achievable product purity. It also affects the economic and energy performance through the ease of separation in the extractive distillation column and through its impact on the CAPEX and operating cost of both connected distillation columns. Design of an extractive distillation process remains a challenge due to its sensitivity to phase behaviour and to thermodynamic properties of multicomponent mixtures formed by the entrainer and the azeotropic pair. In practice, the knowledge of this often relies on models, due to scarcity of data at dilute conditions.

Separation feasibility and total process cost of the extractive distillation process is closely related to two operating parameters, the entrainer flow rate fed to the extractive distillation column and the reflux ratio in each of the two-connected distillation columns. The best entrainer must be chosen such as to perform the separation with a low energy consumption and/or a low total annual cost (TAC), where each criterion may imply different optima (You et al., 2015). Low energy consumption and TAC are essentially related to a small value of the entrainer flow rate F_{Em} (i.e. the easiness of the separation task) and the low values of the minimum reflux ratio, R_m for both distillation columns. Indeed, low entrainer flowrate and low reflux ratio decrease internal flows, and thus the energy consumption and operating costs are reduced. Besides, low entrainer flow rate and reflux ratio are characteristics of an efficient separation, which could usually be carried out with less theoretical stages, lowering the capital costs.Short-cut methods help determine the minimum values of F_{Em} and R_m , in particular by assessing the pinch branches of the liquid profile of the extractive section. Among shortcut methods for continuous operation, different systematic algebraic methods (Levy et al., 1985), the bifurcation theory (Knapp and Doherty, 1994), or the rectification body method (RBM) (Brüggemann and Marquardt, 2004) exist. An elegant algebraic method, with a simplicity suited our purpose, is the Infinitely Sharp Split (ISS) method of Petlyuk, extended from simple distillation (Petlyuk et al., 1999) to extractive distillation (Petlyuk et al., 2015), in order to identify possible splits for different ternary residue curves maps with feasible thermodynamic portraits given by the univolatility curves. The ISS method has been recently applied to optimal conceptual design of extractive distillation process using a dividing wall column (Petlyuk et al., 2021). Petlyuk et al. (2015) highlighted that this method is applicable to conceptual design of distillation columns for separating multicomponent mixtures with several azeotropes. Although it bears some limits, the ISS method enables the calculation of the minimum entrainer flow rate and reflux ratio in a simple way. It is based on a simplified mass balance around the extractive distillation section and only requires a ternary vapour – liquid equilibrium model. Besides, the ISS method delimits

the bundle of the feasible liquid profiles into each column section with a precision comparable to that of other more rigorous methods such as the RBM method.

The short-cut methods mentioned for extractive distillation process design, all require selection of a suitable entrainer. Finding the ideal candidate is not easy because the entrainer must ensure a good separation performance for both connected columns, and possess a set of other properties. Entrainer properties have different impacts on the distillation process. Numerous works have examined the entrainer selection for the extractive distillation column only. As the entrainer should either enhance or reduce the relative volatility α_{AB} in the azeotropic mixture AB, this thermodynamic parameter has been widely used for entrainers ranking. Being based on VLE data, the relative volatility varies with composition but it is usually evaluated for the azeotropic pair, A and B, at infinite dilution $\alpha_A^{\infty E}$.

Other criteria use the selectivity, S_A , evaluated for a pair (A, B) at infinite dilution, i.e.

$$S_{A,B}^{\infty E} = \frac{\gamma_A^{\infty E}}{\gamma_B^{\infty E}} \tag{1}$$

With further verification via rigorous MINLP optimization of the two connected distillation columns minimizing the TAC, Kossack et al. (2008) concluded that $S_{A,B}^{\infty E}$ is a useful parameter but depends on the thermodynamic model, and it is not a very reliable criterion for the entrainer selection in the separation of acetone – methanol mixture, comparing DMSO, water, ethylene glycol and other candidates for recovering acetone as distillate. Momoh (1991) investigated three mixture separations with many entrainers and concluded that $S_{A,B}^{\infty E}$ correlated well with the TAC if the entrainer cost is neglected. Both works pointed out that the selectivity $S_{A,B}^{\infty E}$ criterion overweighs the extractive distillation column cost in the optimal TAC compared to that of the entrainer recovery column, which is strongly dependent on the entrainer boiling point and the vaporization enthalpy. Hence, Kossack et al. (2008) suggested to use the $S_{A,B}^{\infty E} C_B^{\infty E}$ product defined as:

$$S_{A,B}^{\infty E} C_B^{\infty E} = \frac{\gamma_A^{\infty E}}{\gamma_B^{\infty E}} \cdot \frac{1}{\gamma_B^{\infty E}} \tag{2}$$

where $C_B^{\infty E}$ is the entrainer capacity to hold the component B. A better agreement was found between the entrainer ranking defined by the values of $S_{A,B}^{\infty E} C_B^{\infty E}$ and the one found by the TAC minimization for 14 entrainers to separate acetone – methanol mixture (Kossack et al., 2008).

The entrainer ranking based on these criteria often differs from the ranking obtained by subsequent studies, based on process optimization or experiments. Actually, these criteria are only valid for the first extractive distillation column and do not include the regeneration column

operation and cost, although many studies have demonstrated their impact on the optimal operation of the entire extractive distillation process (Gerbaud et al., 2019). This has prompted the investigation of novel and more reliable ranking criteria with a better consideration of the entrainer impact over the two connected distillation columns.

An alternative ranking has been proposed using the thermodynamic criteria that are directly related to the topology of the ternary composition space of the vapor-liquid equilibrium. Acknowledging the coincidence of the univolatility curves intersection $x_A^{\alpha_A\ -1}$ at the binary side in the ternary residue curve maps and the value of the minimum entrainer flowrate under pinch conditions, several authors used the $x_A^{\alpha_A\ -1}$ value as an entrainer selection criterion (Laroche et al., 1991, 1992a,b, Lelkes et al., 1998). Another valuable criterion is to compare entrainers according to their driving force D (Gani and Bek-Pedersen, 2000) characterizing the ease of separation. D_A^A (resp. D_B^B) is defined as the maximum value of the difference $y_A - x_A$ (or $y_B - x_B$) over the AE (reps. BE) composition range.

Cignitti et al. (2018, 2019) used both criteria in solving a CAMD problem finding suitable high boiler homogeneous entrainer for the acetone – methanol separation, by considering D_A^A and D_B^B in the objective function to be maximized, while constraining the entrainer composition of the isovolatility curve $x_E^{(\alpha_{A,B}-1)}$ and $x_E^{(\alpha_{A,B}-2)}$. Although ethylene glycol (EG) and DMSO exhibited similar isovolatility curve maps and $x_A^{\alpha_A\ -1}$values similar to the best benchmark entrainer, driving forces D_A^A and D_B^B where greater for EG. Short-cut rankings were compared to process simulation results based on optimization studies of either the process energy consumption or TAC resulting. Optimization results validated the ranking based on maximal driving forces under $x_E^{(\alpha_{A,B}-1)}$ or $x_E^{(\alpha_{A,B}-2)}$, but optimization results invalidated rankings based on criteria $S_{A,B}^{\infty E}$ or $S_{A,B}^{\infty E} C_B^{\infty E}$.

In these works, the key operating parameter R_m is left out of comparison of entrainers. In this paper a more robust criterion for entrainer selection is developed by coupling the ISS method (Petlyuk et al., 2015) with other criteria used by Cignitti et al. (2019) such as the entrainer composition x_E at intersection point of the curve $x_A^{\alpha_A\ -1}$ (Hsu et al., 2010, Gerbaud et al., 2019) and the separation driving forces D_A^A and D_B^B, defined as $D_i^i = (y_i - x_i)_i$ (Gani and Bek-Pedersen, 2000). Indeed, the coupling of these criteria enables the evaluation of the entrainer impact in both columns of the extractive distillation process. Entrainer ranking can be performed by comparing the limiting values F_{E_m} and R_m of the extractive distillation column or the D_A^A and D_B^B values related to the efficacy of the two connected distillation

columns. Besides, F_{Em} computed with the ISS method will allow to check whether the intersection of the univolatility curve $x_A^{\alpha_A=1}$ is a relevant criterion. In this work, this methodology is applied to the most common and relevant separation case in industrial practice concerning the separation of the minimum-boiling azeotropic mixture with high boiling entrainers. The ternary residue curve map corresponds to the class 1.01-a having a 21.6% occurrence among the 26 total ternary diagrams belonging to the Serafimov classification.

The paper is organized as follow: Section 2 briefly describes the ISS method as well as the methodology developed for entrainer screening and the two-column process optimization procedure. Section 3 presents the application of the new combined approach to rank a group of entrainers already studied in literature for the separation of methanol – dimethyl carbonate mixture by extractive distillation. Among the numerous authors who investigated suitable entrainers for this separation, we focus on Hu and Cheng's work who carried out experimental measurements of activity coefficients and developed a consistent set of thermodynamic models for comparing entrainers from a list of 35 organic compounds (Hu and Cheng, 2017). We compare our entrainer ranking obtained with an integrated shortcut method with their short list, and discuss the simulation results based on the minimization of the TAC of the process with the extractive column and the entrainer regeneration column.

2. Application of the Infinitely Sharp Split (ISS) method for entrainer screening

2.1. ISS Method Overview

The ISS method assumes that the column works under constant molar flow rates, and each column section has an infinite height (Petlyuk et al., 2015). One azeotropic compound (A or B) is absent at the entrainer feeding tray whereas the other one (B or A) is in the bottom product. Fig. 2a shows how the compounds split inside the extractive distillation column for a high boiling entrainer interacting with B whereas A is withdrawn in the distillate product. The separation of a ternary mixture A-B-E takes place in the extractive distillation column if the extractive liquid profile (ELP) in the extractive section crosses both the rectifying and the stripping liquid profile. Indeed, the feasible extractive region (FER) contains all ELP starting at the same lowest temperature point (unstable node N_e^-), approaching the same intermediate temperature point (saddle S^E) and arriving at the same highest temperature point (stable node N_e^+) placed on the edge AE. For a given reflux ratio (L/V), the FER is limited by a particular ELP passing through the three singular points N_{e1}^-, S^E and N_e^+ that is usually called boundary of the feasible extractive region (BFER).

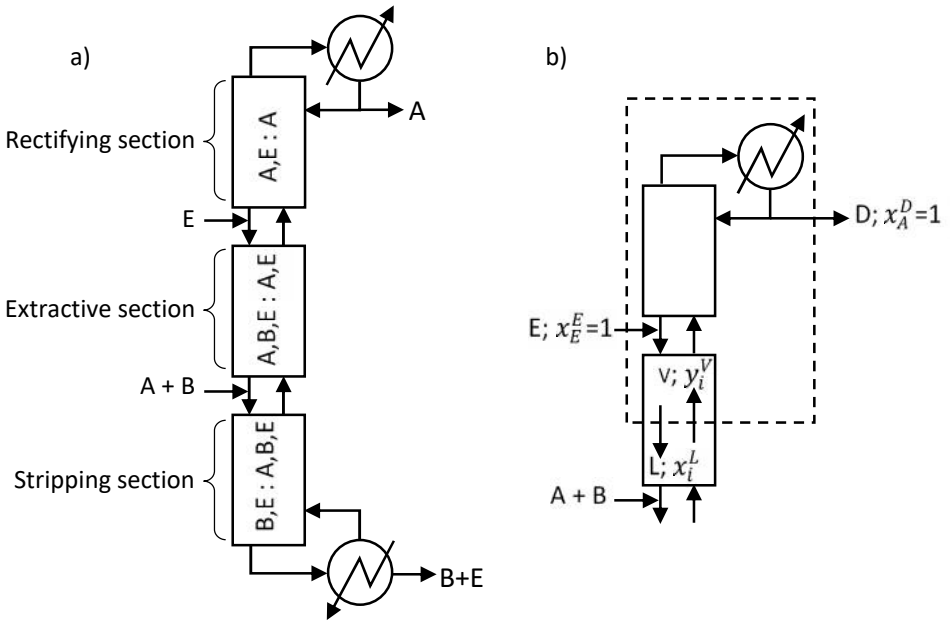

Fig. 2 (a) Distribution of components along the height of extractive distillation column according to the ISS method. (b) Rectifying and extractive column section material balance.

Fig. 3 displays several BFER corresponding to a molar flow rate ratio entrainer/distillate $(E/D) = 1.9$ at different reflux ratios (L/V) for the ternary mixture acetone – methanol – water (Seihoub, 2018). These BFER were computed by using the ISS method with the thermodynamic model proposed by Petlyuk et al. (2015). A single variation of (L/V) at a fixed (E/D) will change the location of the saddle point S^E and the size of the BFER. The trajectory passing through all saddle points S^E corresponds to the first pinch branch that connects the B vertex with the root x_A^{r1} located on the AE edge. The shaded region displayed in Fig. 3 is a total feasible extractive region (TFER) that contains all ELP calculated for the same $E/D = 1.9$ and $L/V = 0.8$ with different compositions inside the extractive section. Any extractive liquid profile within this region intersects at one end with the rectifying liquid profile that lies near the AE edge and passes through the distillate composition. The other end of the extractive profile crosses the liquid profile of the stripping section that ends at the edge BE. Computation of an ELP can be done by using the differential mass balance (Levy et al., 1985). The TFER of the ternary system is usually composed by two FER, I and II (in Fig. 3), where all ELP share the same N_e^+ and saddle S^E but start at different unstable nodes N_{e1}^- (FER I) and N_{e2}^-(FER II). Both regions are divided by the extractive boundary (EB) connecting N_e^+ and saddle S^E (dashed line in Fig. 3). It should be noted that N_{e2}^- lies outside the edge AB. Indeed, feasible values of E/D and L/V are related to the existence of both N_e^+on the edge AE and S^Einside the composition simplex (Knapp and Doherty, 19945). Petlyuk et al. (2015) showed that the minimum value of (L/V) in the extractive section occurs when S^E and x_A^{r1} are coincident on the edge AE for a

given (E/D). When $(L/V) = (L/V)_m$, S^E vanishes and there is no connection between the extractive liquid profile and the rectifying liquid profile on the edge AE. Similarly, the root x_A^{r2} of the second pinch branch coming from the azeotrope AB_{azeo} is associated with the maximum value of $(L/V)_m$ for the same (E/D). Both roots move towards each other when (E/D) decreases and at the minimal value $(E/D)_m$ x_A^{r1} and x_A^{r2} coincide on the edge AE. Further reduction of (E/D) moves the singular point N_e^+ inside the ternary diagram making disappear the intersection between the extractive and the rectifying liquid profiles on the edge AE. In practice, the operating (L/V) is computed using $(L/V)_m$ for an operating $(E/D)_o$ around 1.5-2 times of $(E/D)_m$ but this heuristic may be adapted to each specific separation problem (Knapp and Doherty, 1994).

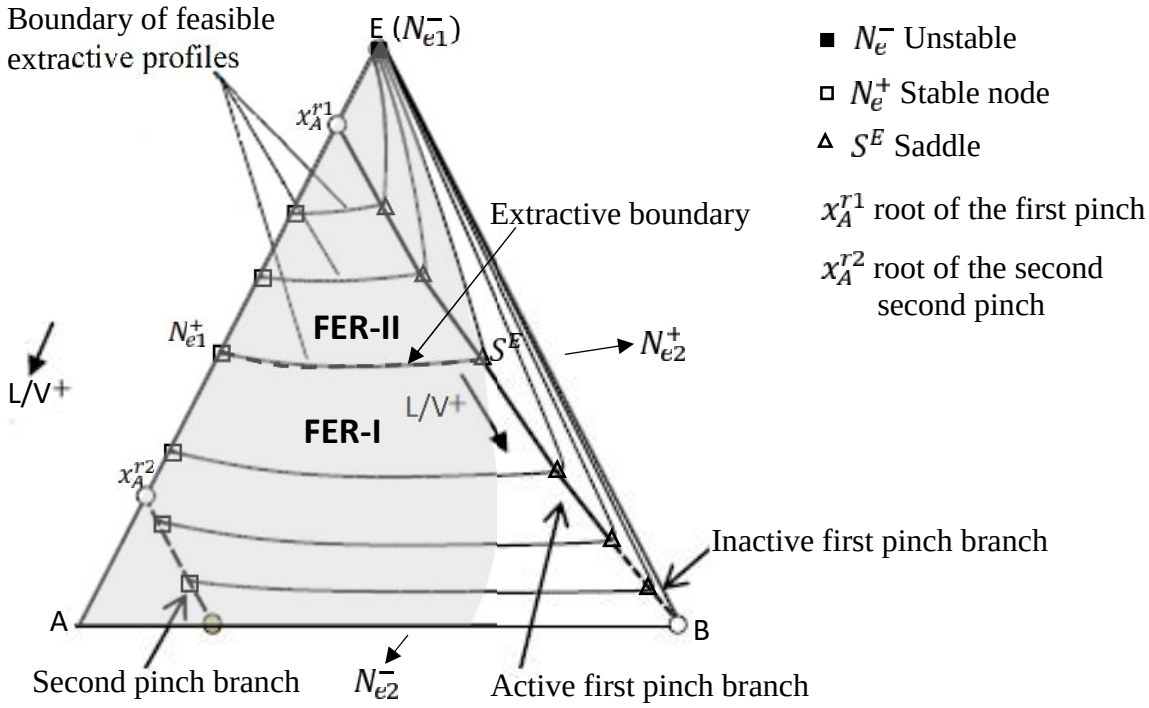

Fig. 3 Feasible extractive regions and pinch branches for the acetone(A) – methanol(B) – water(E) at (E/D)=1.9 at different reflux ratios L/V in the extractive section. (Seihoub, 2018)

The ISS method is based on a simplified mass balance around the combined rectification and extractive sections (Fig. 2b) under the assumption of constant molar flow rates and the infinite height of each column section (Petlyuk et al., 2004, 2015). The material balance is set considering that the stable node N_e^+ is located at the extractive tray on the edge AE where B is the absent compound. The molar fraction of A at N_e^+ satisfies $x_A^{m+1} = x_A^m$ under pinch conditions in the extractive tray, that is $(L/V) = (L/V)_m$. In addition it is supposed that x_A^D = 1; $x_B^D = x_E^D = 0$ (pure distillate assumption) and $x_E^E = 1$, $x_A^E = x_B^E = 0$ (pure entrainer assumption).These assumptions lead to the following system of equations:

- Mass balance of B (absent compound on the edge AE)

$$V.K_B^T.x_B^T = L.x_B^T + D.x_B^D - E.x_B^E = L.x_B^T$$

$$\frac{L}{V} = K_B^T \quad (3)$$

- Mass balance of A for computing the delta point x_A^Δ as a difference between the entrainer feeding and the distillate product

$$\Delta = D - E$$

$$(D-E).x_A^\Delta = D.x_A^D - E.x_A^E = D$$

$$E/D = \frac{x_A^\Delta - 1}{x_A^\Delta} \quad (4)$$

- Mass balance for component A at the root point x_A^T on the edge AE to set a relationship between x_A^T and x_A^Δ

$$V.K_A^T.x_A^T = L.x_A^T + D.x_A^D - E.x_A^E = L.x_A^T + (D-E).x_A^\Delta$$

$$x_A^\Delta = \frac{(K_A^T - K_B^T)}{(1-K_B^T)} x_A^T \quad (5)$$

- Relationship between $(L/V)_t$ at the rectifying section with $(L/V) = K_B^T$ computed for the extractive section

$$\frac{L}{V_T} = \frac{K_B^T - \frac{E}{D}}{1 - \frac{E}{D}} \quad (6)$$

Some important observations can be made from the Eqs. (3-6):

- According to Eq. (3), the L/V in the extractive section is equal to the distribution coefficient of the absent compound B at a given (E/D);
- $(L/V)_m = K_B^{\infty A}$ (x_A^{T1}) at the root point of the first pinch branch x_A^{T1} is located at the edge AE, because the points S^E and x_A^{T1} merge with each other providing a FER with zero surface. When $(E/D) > (E/D)_m$, Petlyuk et al. (2015) also demonstrated that $(L/V)_m = K_B^{\infty A}$ (x_A^{T2}). Hence, the Eq. (5) have two roots satisfying the condition $x_A^{T1} < x_A^{T2} < x_A^{\alpha A=1}$;
- According to the Eq. (4), $(E/D)_m$ corresponds to the minimal value of x_A^Δ;
- Scanning the molar fraction x_A^A of A on the edge AE, both trajectories E/D and x_A^Δ versus x_A^A can be computed from Eqs. (4) and (5), enabling the identification of

$(E/D)_m$. The corresponding value of $K_B^{\infty A}$ ($x_{A,m}^r$) is the $(L/V)_m$ of the extractive section at $(E/D)_m$.

It must be noted that the description of the ISS method discussed above is only valid for an extractive distillation process corresponding to the Serafimov's ternary diagram classes 1.0-1a-m1 and allowing separation of minimum-boiling azeotropic mixtures using high boiler entrainers that interact preferably with B. The mass balances given by Eqs. (3-5) can be easily modified when using the same type of entrainers showing a stronger interaction with A (class 1.0-1a-m2). In this case, A is the absent compound on the edge B-E. However, the Serafimov's ternary diagram classes 1.0-1b, 1.0-2, and 0.0-1 also describe feasible residue curve maps enabling the separation of close boiling mixtures and azeotropic mixtures with all entrainer types by extractive distillation classes. A complete compilation including the feasibility conditions, expected products and limiting operating conditions has been reported by Gerbaud et al. (2019). Some important modifications must be made to apply the ISS method to other extractive distillation types that might require a different configuration for the extractive distillation column. For instance, the feeding of the low boiling entrainer in a tray located below that of the minimum-boiling azeotropic mixture to be separated by still using two connected distillation columns. Applying the ISS method to a given column configuration first requires defining the feasible region for each section of the extractive distillation column based on the order of the distribution coefficients. Next, the absent compound of the ternary mixture must also be defined. Finally, mass balances assuming infinite height of each section can be deduced, allowing the computation of the $(E/D)_m$ and R_m . The driving force concept can be applied to all types of extractive distillation.

2.2. Pinch branch computation

Petlyuk et al. (2015) highlighted that at $(E/D)_m$ the first and the second pinch branch can meet each other at $x_{A,m}^r$ = x_A^{r1} = x_A^{r2} on the binary edge AE. Furthermore, different configurations of the first and second pinch branch at $(E/D)_m$ and $(L/V)_m$ occur even for the most used Serafimov ternary class 1.01-a. U-shape pinch branches (Petlyuk et al., 2015) touch each other on the AE edge at $x_A^{r,m}$. , The pinch branches merging at $x_A^{r,m}$ happen in ternary diagram characterized by the $(L/V)_m$ value higher than those related to U-shape patterns (Petlyuk et al., 2015). . In fact, $(L/V)_m$ is equal to the distribution coefficient K_B^r of the absent component at the intersection point. The mathematical methodology used for this work allows to compute the intersection point between both pinch branches wherever it occurs. The computation is based on the following idea.

The pair of algebraic conditions associated with the equilibrium condition

$$K_A\, x_A + K_B\, x_B + K_E x_E = 1 \tag{7}$$

and the pinch condition Eq.(5) for a given value of x_A^{Δ} is

$$x_A^{\Delta}(1 - K_B) = (K_A - K_B)x_A$$

It describes two surfaces in the full 3D temperature – composition state space of the system. Their intersection defines a smooth curve in this 3D space. The tangent vector field to this curve defines a system of three ordinary differential equations (ODE) for the temperature and the components molar fractions. If the point x_A^T is already found by the method described in the next section, the whole pinch branch starting from this point can be computed by integration this ODE system by any conventional ODE solver with desired precision. Such an algorithm was already successfully implemented to compute the univolatility curves in Shcherbakova et al. (2017a, 2017b, 2018) and Cots et al. (2021, 2017b, 2018). The described computational method requires to access the derivatives of the thermodynamic model. This difficulty can be overcome by using either a numerical tool allowing symbolic computations (as Mathematica® used in this paper) or an automatic differentiation library as proposed by Cots et al. (2021).

2.3. Methodology for entrainer screening

Application of the ISS method requires selection of a suitable model of the vapor – liquid equilibrium for the ternary mixture ABE as well as a model for computing the vapor pressure of each pure compound. Once this is done, the methodology for entrainer screening, involves the following steps:

a) Calculation of the $x_A^T = x_{A,m}^T$ that minimizes the objective function corresponding to (E/D) value, which can be obtained by the combination of Eq. (4) and Eq. (5). It should be noted that $x_{A,m}^T$ is always located between $x_A^A = 0$ and the value of $x_A^M = x_A^{(\alpha_{A,B}=1)}$ corresponding to the point of the univolatility curve on the edge AE. So, $x_{A,m}^T$ is the solution of:

b)

$$\min_{x_A^T, T}\left[1 - \frac{(1 - K_B)}{x_A^T(K_A - K_B)}\right] \tag{8}$$

subject to

$$\sum_{i-1}^{3} K_i x_i^T - 1 = 0\,, \qquad 0 < x_A^T < x_A^M \quad , \quad x_B^T = 0$$

This problem was solved using Mathematica 9.

c) Set $(L/V)_m = K_B^{\infty A}(x_{A,m}^r)$ of the extractive section. Note that $K_B^{\infty A}(x_{A,m}^r) = K_B(x_{A,m}^r)$ at the minimum value of Eq. (8).

d) Calculate the minimum reflux R_m for the rectifying section using $(L/V)_m = K_B^r(x_A^r, T)$.

e) Set the potential candidate list with the entrainers providing low values of $(E/D)_m$ and R_m .

2.4. Sequential optimization procedure

The extractive process optimization is an MINLP problem with continuous variables such as entrainer flowrate or reflux ratio, while the column tray number and feed location are integer variables. Many solution strategies exist, including combination of stochastic and deterministic algorithms (García-Herreros et al., 2011, Skiborowski et al., 2015). In this work the MINLP problem is solved as a TAC minimization problem by using a sequential optimization methodology (de Figueirêdo et al., 2011, Luyben and Chien, 2010, You et al., 2014, 2015).

We study the extractive distillation of the minimum-boiling azeotrope mixture methanol (A) – dimethyl carbonate (B), with a heavy entrainer (E). For a given entrainer, one first runs simulations with ASPEN V10 of the whole process flowsheet, including both the extractive distillation (ED) and the entrainer regeneration (ER) columns (Fig. 1). Table 1 shows the distillate flow rates, product molar purity and recovery yields used in the simulation. The purity target for DMC satisfies the pharmaceutical grade requirements. The nearly pure methanol purity specification is taken equal to the one used in the literature (Hu and Cheng, 2017, Varyemez and Kaymak, 2022). Initial process feasible operation conditions satisfying the constraints were found using the published results for the extractive distillation of methanol – DMC (Hu and Cheng, 2017, Varyemez and Kaymak, 2022). Both feed streams are inserted at 54°C, as prescribed by Varyemez and Kaymak (2022) who suggested this value it as suitable choice for heat integration, which is not carried out in this work. One can take into account another criteria that lead to a feasible extractive distillation (Gerbaud et al., 2019): typically, the component B should be presented as less as possible on the entrainer feed tray, such that the extractive section composition profile can intersect the rectifying section profile that enables to the component A distillate purity specification to be satisfied. Besides, component A recovery yield should be as high as possible, such that nearly no A leaves the bottom of the extractive column to enter the regeneration column. The regeneration column then behaves like a binary column for which heuristics are available, including Petlyuk's ISS method for a single feed column (Petlyuk, 2004). Such a preliminary simulation provides feasible values for the feed flow rate, reflux ratio for each column, the total stage numbers for each column and other

process operating parameters such as tray numbers, feed tray locations and distillate flow rates values. Cooling water (303.15 – 318.15K) is used in column condenser and for cooling the recycled entrainer. Depending on each entrainer characteristics, high, medium or low-pressure steam used in the boiler will be specified later.

Table 1. feed stream characteristics and constraints for the extractive distillation process.

Feed			**Distillate requirements**		
F_A	170.5	kmol/hr	D_1	145.5	kmol/hr
P	101325	Pa	D_2	25.1	kmol/hr
T_{FAB}	327.15	K	$x_{D1, MeOH}$	≥ 99.99	mol%
T_{FE}	327.15	K	$x_{D2, DMC}$	≥ 99.5	mol%
$x_{FAB, MeOH}$	85.33	mol%	yield $_{D1, MeOH}$	≥ 99.998	%
$x_{FAB, DMC}$	14.67	mol%	yield $_{D2, DMC}$	≥ 99.5	%

First, the sequential optimization procedure described in Figure 4 is followed, starting from the feasible process simulation satisfying all constraints. For a given total number of trays N_1 (extractive distillation C1 column) and N_2 (entrainer regeneration C2 column), the simulation of the open-loop flowsheet with no entrainer recycle is optimized under product purity and recovery constraints by the sequential quadratic programming (SQP) method built into the Aspen simulator. The variables are both the entrainer flow rate F_E and columns reflux ratios R_1 and R_2. The initial values for N_1 and N_2 were taken from Hu and Cheng (2017), while initial guesses for entrainer feed flow rates and reflux ratios have been taken considering the ISS method, and were continuously varied in a range that goes: a) from FE_{min} to 3 FE_{min} , FE_{min} being the minimum entrainer feed flow rate; lower values of FE_{min} are not feasible, while the values higher than $3FE_{min}$ are related to higher energy consumptions, corresponding therefore to the TAC out of interest for an optimization; b) from 0.2 to 20 for both reflux ratios so as to avoid local minima.

Secondly, a sensitivity analysis is performed in several steps to find the optimal values of the total feed trays and the three feed tray locations NF_{AB}, NF_E and NF_{SR}. Achieving minimum TAC at each step is the decision criterion to carry out to go to the next step. TAC including capital cost per year (CAPEX) and operating costs (OPEX), with a payback period of 3 years (8200 hrs) is evaluated as

$$TAC = \frac{capital\ cost}{payback\ period} + operating\ costs \tag{9}$$

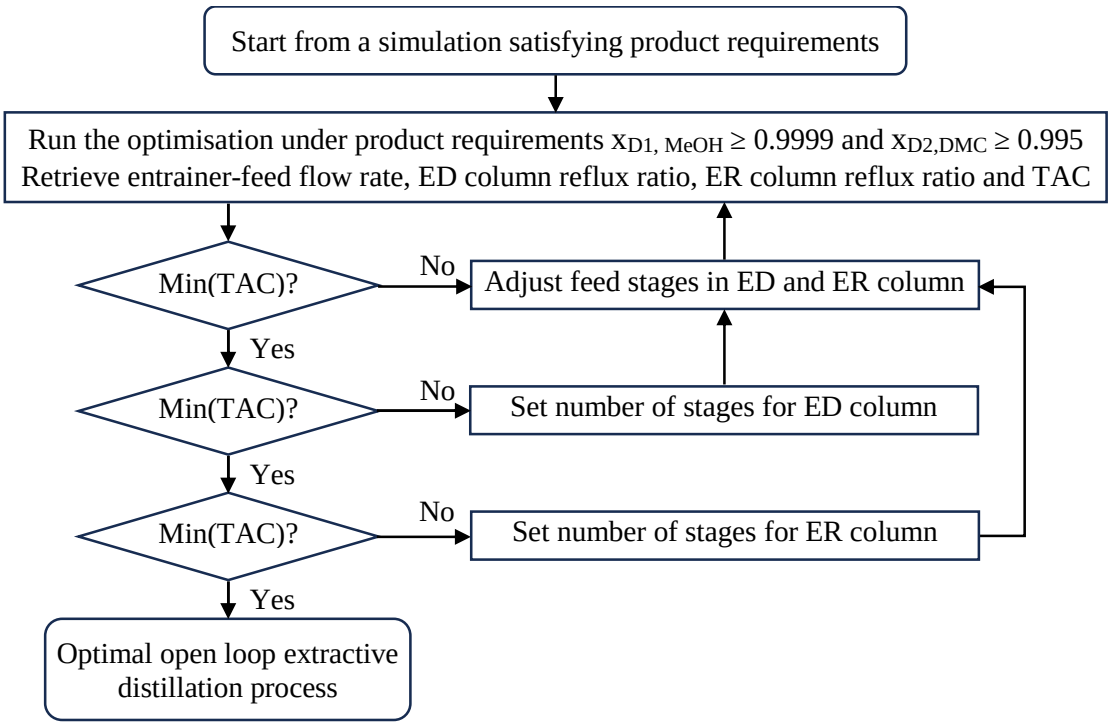

Fig. 4. Sequential optimization procedure

The operating and capital cost information is taken from Varyemez and Kaymak (2022) who studied the extractive distillation of DMC-methanol with MIBK, except for the column height and steam costs taken from supplementary information published by Gu et al. (2018).CAPEX only includes the column shell, the equilibrium trays and the heat exchangers. The column shell cost depends on both height and diameter of the column. OPEX comprises the cooling water (0.34 $/GJ) and the steam at low (7.72 $/GJ), middle (8.22 $/GJ) and high pressure (9.88 $/GJ). The price of the entrainer in the OPEX is not considered because its impact on the economic feasibility of the process depends on the optimal entrainer flowrate. Besides, the price and availability in the global market can change significantly in a short period when demands increase exponentially. The column operates at atmospheric pressure, which is the pressure at the condenser. No pressure drop is considered.

The optimization procedure is carried out in an open loop, i.e. fresh and pure entrainer is fed to the extractive distillation column with a flowrate matching the entrainer flowrate leaving the bottom of the entrainer recovery column. The optimal open-loop solution is further tested for convergence in a closed-loop simulation, where the entrainer main feed is supplied by the recycled entrainer stream. In sequential optimization, running closed-loop simulation may lead to convergence problems. This is not only due to numerical problems, but also due to physical issues. Indeed, owing to the entrainer recycle stream, D_1 and D_2 flow rates are strongly interconnected with each other. You et al. (2016) showed that an unreasonable choice of distillate flow rate may lead to poor product quality and / or enhance the difficulty of the

separation, requiring more energy and cost to achieve the same product recovery. They also showed that it sets limits on the entrainer recycle stream and its impurity content, and that sometimes a higher recovery yield may cost less energy. The stability of the selected optimal point was corroborated by sensitivity analysis by changing by one (below and above) the position of each feeding in both distillation columns.

3. Case Study

3.1. Separation of methanol – dimethyl carbonate using a heavy entrainer

We investigate the extractive distillation with a heavy entrainer (E) of the minimum-boiling azeotrope methanol (A) – dimethyl carbonate (B), which leads to the familiar ternary residue curve map class 1.0-1a. Its industrial interest appears in several novel technologies to produce dimethyl carbonate (DMC) from both usual chemical pathways, namely the methanolysis of urea or propylene carbonate (Huang et al., 2021). Note that the azeotrope is persistent up to 30 bars (Matsuda et al., 2019) so, feasible and attractive alternatives using pressure-swing distillation have been compared with extractive distillation process using MIBK as entrainer (Yang et al., 2019; Varyemez and Kaymak, 2022).

Many entrainers have been proposed for this separation by extractive distillation at atmospheric pressure. For example, Hsu et al. (2010) investigated aniline, ethylene glycol and phenol as entrainers, using a fast screening approach based on univolatility curve analysis and volatility increase, combined with process simulation. Hu and Cheng (2017) developed a three-tiered holistic approach for the optimal synthesis and design of extractive distillation for separating methanol (A) from dimethyl carbonate (B). The preliminary entrainer screening was based on selectivity values at infinite dilution computed by Eq. (1) using Modified UNIFAC Dortmund and COSMO-SAC. The initial list of entrainers includes 35 organic compounds (alcohols, ketones, ethers, esters, amines, amides) commonly studied in literature for the separation of minimum-boiling temperature azeotropes. Among them, 12 entrainers increasing significantly $S_{A,B}^{\infty E}$ were selected, including two new compounds, ethyl benzoate and methyl salicylate, never investigated before. Some other compounds were already studied in the literature like phenol (Wang et al., 2010, Hsu et al., 2010), dimethyl oxalate (Ma et al., 2004), 2-ethoxyethanol (Matsuda et al., 2011) and 4-methyl-2-pentanone (Matsuda et al., 2011). The entrainer efficacy was assessed by process simulation using Aspen Plus for the six most promising entrainers ranked with respect to minimum TAC of the extractive distillation process with both the extractive distillation column and the entrainer regeneration column.

Hu and Cheng (2017) carried out experimental measurements of activity coefficients and developed a consistent set of thermodynamic models. We will investigate five of their final list of entrainers, namely methyl salicylate, phenol, MIBK, ethyl benzoate and 2-ethoxy-ethanol.

3.2. Computation of selection criteria

The method we propose is based on the ISS method coupled with the analysis of the entrainer composition x_E at the intersection point with the curve $x_A^{\alpha_A = 1}$, and the maximum value of the driving force of the binary mixture AE (D_A^M) and BE (D_B^M). It is also compared to the selectivity $S_{A,B}^{\infty E}$. These criteria require vapor-liquid equilibria data that are modelled as follows. Ideal gas behaviour is assumed due to the low operating pressure. The nonideality of the liquid phase is described by the non-random two-liquid (NRTL) model with binary interaction parameters reported by Hu and Cheng (2017).

Figure 5 shows that for each entrainer, methyl salicylate, phenol, MIBK, ethyl benzoate and 2-ethoxy-ethanol, the univolatility curve starts at the binary azeotrope and arrives at the AE edge ($x_A^{\alpha_A = 1}$), indicating that methanol will be drawn as distillate product of the extractive distillation column for all entrainers (Gerbaud et al., 2019). The isovolatility curves were calculated using the method developed by Shcherbakova et al. (2017a). It is worth noting that even though all five entrainers display $x_A^{\alpha_A = 1}$ values close to each other, there is a great diversity iso-volatility curve maps topology, and the maximum value of the α_A does not always happen close to the entrainer vertex. The isovolatility-curve map of methyl salicylate shows a saddle point and the increasing of the isovolatility values occurs when they move towards the vertex B for all entrainers.

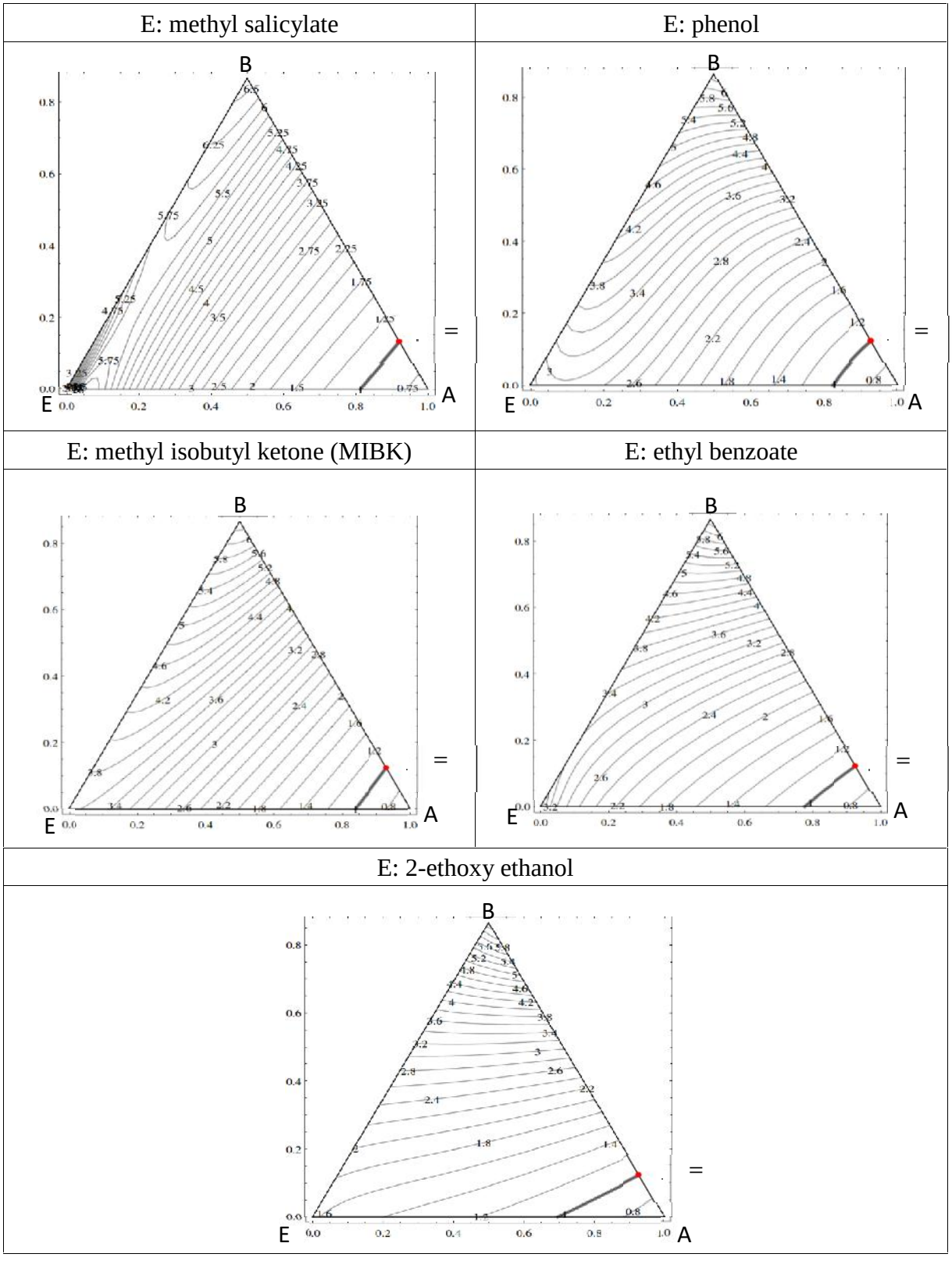

Fig. 5. Isovolatility curve map of the ternary mixture methanol(A) – dimethyl carbonate(B) – entrainer(E) at 1 atmosphere for five entrainer candidates.

The values $(E/D)_m$ and R_m displayed in Table 2 were computed by the ISS methodology described in Section 2. The pinch branches of the extractive distillation column are displayed in Fig. 5 for three values of (E/D). They were found the geometrical computational method described in Section 2.2.

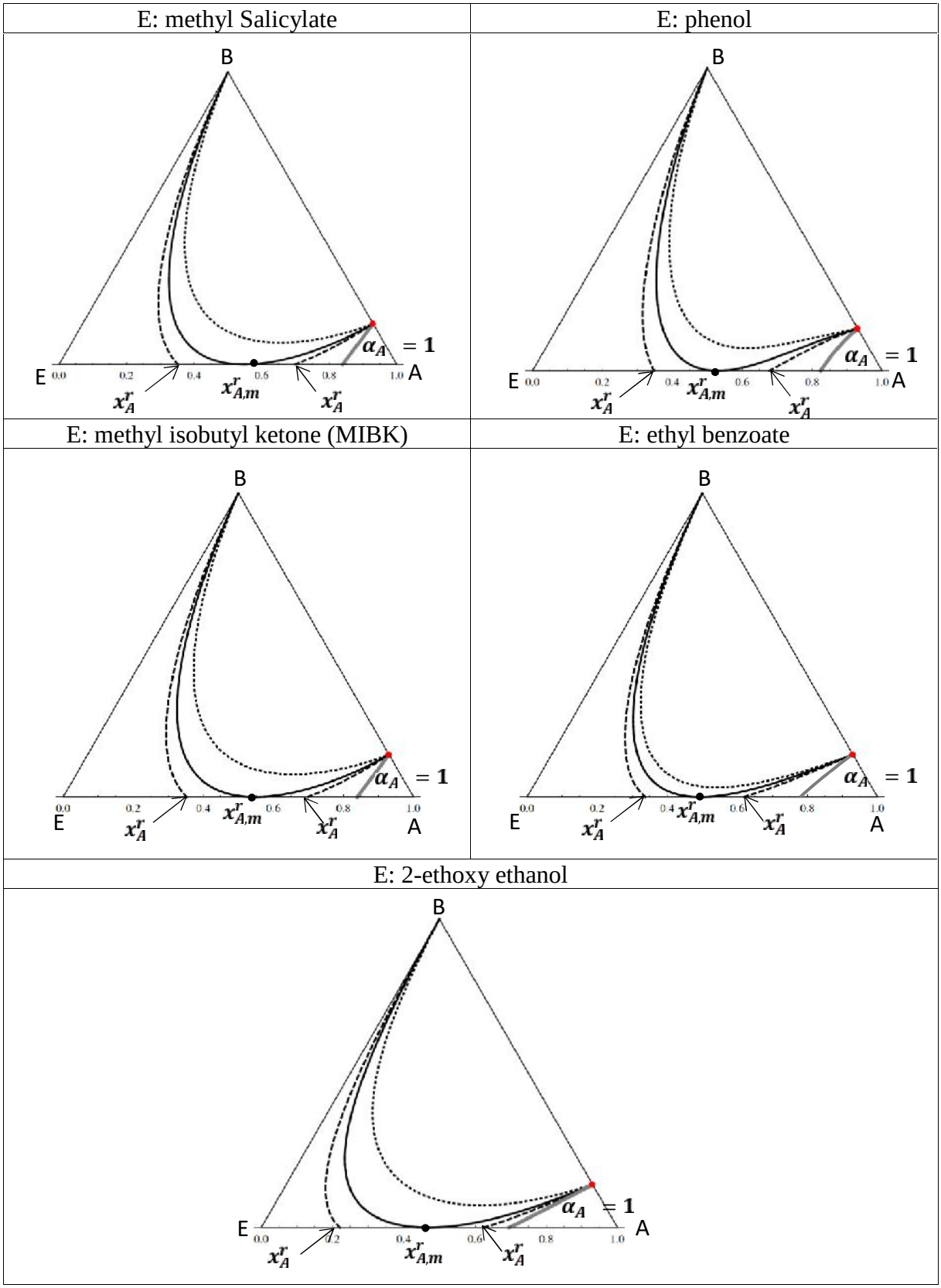

Fig. 5. Pinch branches for several (E/D)*:* ——— $(E/D)_m$, – – – – $(E/D) < (E/D)_m$, ------- $(E/D) > (E/D)_m$

We observe that all pinch branches in Fig. 5 follows the U-shape type, and they touch each other at $x_{A,m}^r = N_{e1}^+$ for $(E/D)_m$. When $(E/D) < (E/D)_m$ these pinch branch moves inside the ternary diagram forming a unique pinch branch linking the B vertex with the

azeotrope AB. Hence, the extractive distillation process is infeasible because the saddle point S^E vanishes and no pinch branch connects the vertex B with the extractive element on the edge AE at the singular point N_{e1}^{+}. Feasible extractive distillation regions like regions FER-I and FER-II (see Fig.3) appear for $(E/D) > (E/D)_m$ because all extractive profiles arrive to the stable node N_{e1}^{+}. The minimum and maximum reflux ratio satisfy the Eq.(3) where $(L/V)_M = K_B^T(x_A^{T1}, T)$ and $(L/V)_M = K_B^T(x_A^{T2}, T)$.

VLE data also allows computation of the selectivity $S_{A,B}^{\infty E}$, and the driving forces D_A^M and D_B^M and the limiting operating parameters $(E/D)_m$ and R_m. Table 2 displays the selectivity values $S_{A,B}^{\infty E}$ at infinite dilution of the entrainer computed by Hu and Cheng (2017) using Modified UNIFAC Dortmund or COSMO-SAC models, and the $S_{A,B}^{\infty E}$ values that we calculated by using the NRTL with the same binary parameters as employed with the ISS approach ($S_{A,B}^{\infty E\check{A}}$).

Table 2: Criteria for entrainer selection for extractive distillation

Entrainers	T_b (K)	$S_{A,B}^{\infty E*,H}$	$S_{A,B}^{\infty E\zeta,H}$	$S_{A,B}^{\infty E}$	$x_A^{\alpha_A=1}$	D_A^A	D_B^B	$(E/D)_m$	R_m
methyl salicylate	493.9	1.438	8.102	0.741	0.8130	0.8080	0.7059	0.9360	0.6769
phenol	455	2.123	2.651	0.934	0.8239	0.7010	0.5379	1.0965	1.2890
MIBK	390.5	0.982	1.385	1.372	0.8392	0.4934	0.2146	0.6745	1.5244
ethyl benzoate	486.55	2.381	3.755	1.228	0.7768	0.8302	0.7036	1.9332	1.9284
2-ethoxy ethanol	408.15	1.625	0.683	0.607	0.6961	0.5390	0.3863	5.0050	5.3760

HC: Hu and Cheng (2017); * Modified UNIFAC Dortmund; ζ COSMO-SAC; NRTL in this work

3.3. Criteria comparison for entrainer selection

Aiming at recovering A as distillate product for (1.0-1a) extractive separation class, an ideal entrainer should enhance volatility of A over B (high selectivity $S_{A,B}^{\infty E}$). Consequently, it should exhibit the univolatility curve passing as close as possible to the point $x_A^{\alpha_A=1}$, give high driving forces D_A^A and D_B^B and low operating parameters entrainer flowrate $(E/D)_m$ and reflux ratio R_m. However, in practice it is not straightforward to rank entrainers on this basis. In Table 2, $S_{A,B}^{\infty E}$ values predicted with the three models are quite different. Besides, it brings out some unexpected results. Firstly, the $S_{A,B}^{\infty E}$ value depends on the thermodynamic model: Ethyl benzoate or methyl salicylate or MIBK exhibit the highest $S_{A,B}^{\infty E}$ value when using Modified UNIFAC Dortmund or COSMO-SAC or NRTL, respectively. Secondly, NRTL-based $S_{A,B}^{\infty E}$ is less than unity for the methyl salicylate and phenol, which means that the volatility of B is enhanced and DMC would then be the distillate. However, this is inconsistent as both entrainers

are meant to provide methanol (A) as distillate product of the extractive column because their respective univolatility curves end at the edge methanol – entrainer (Fig. 4), as later verified by simulation. Consequently, the $S_{A,B}^{\infty E}$ value is not a reliable criterion and will be not considered further for entrainer screening.

Concerning $x_A^{\alpha_A = 1}$, the intersection point of the univolatility curve on the edge methanol – entrainer, all entrainers have a similar value of $x_A^{\alpha_A = 1} \approx 0.8$, except 2-ethoxy ethanol near 0.7. Hence no clear decision can be made. Usually, high values of $x_A^{\alpha_A = 1}$ closer to the A vertex are associated with the minimum entrainer flow rate for batch extractive distillation (Lelkes et al., 1998) and continuous extractive distillation (Shen et al. 2013). Regarding $(E/D)_m$ computed by the ISS method in Table 2, phenol's value is ~ +80% that of MIBK for very similar values of $x_A^{\alpha_A = 1}$. So, this heuristic does not hold here. Further, Hsu et al. (2010) point out that the whole isovolatility map must be analysed. Investigating the extractive distillation of DMC – methanol with either aniline, phenol or ethylene glycol (EG), they note that although EG had the highest $x_A^{\alpha_A = 1}$ value, it did not enhance volatility between DMC and methanol as much as phenol or aniline did and simulation showed that aniline process led to lower TAC. Cignitti et al., (2019) reached a similar conclusion for the extractive distillation of acetone – methanol azeotrope with ethylene glycol (EG), computing values of $x_A^{\alpha_A = 1}$ using different thermodynamic models.

Transposed to our case study, the portrait of the isovolatility lines in Fig. 4 infers that methyl salicylate could provide a lower $(E/D)_{min}$ because the univolatility curve intersects the edge A-E closer to the A vertex. However, this is not confirmed by the $(E/D)_m$ computed with the ISS method (Table 2).

Regarding the other remaining criteria in Table 2, one can acknowledge that it is difficult to rank entrainers based on only one criterion or using a weighted sum of them. Bearing in mind the ideal candidate characteristics enunciated at the beginning of this section (high driving forces, low reflux and low entrainer flowrate), one can propose to combine ISS parameters and driving forces. Usually, an entrainer having small value of $(E/D)_m$ and high driving forces with the azeotropic compounds allows separation with a shorter column and low energy demand. Large values of driving force D_A^A facilitates separation of A in the rectifying section of the extractive distillation column. Similarly, a large D_B^B eases the entrainer regeneration from the B-E mixture entering the regeneration column. Also, good economic and energy performance of the extractive distillation column must be influenced by a ratio of driving forces D_A^A / D_B^B due to the competitive separation of A and B in the extractive and in the stripping sections of the extractive distillation column Cignitti et al. (2019). Cignitti et al. (2019)

highlighted that an optimal ratio D_A^A / D_B^B near 1.2 was correlated with a low TAC and a low total energy consumption design from the comparison of three entrainers (water, DMSO and ethylene glycol) for separation the azeotropic mixture acetone – methanol. The analysis of the R_m impact is more ambiguous because the optimal reflux ratio depends on the number of equilibrium trays and the entrainer flow rate. Entrainer ranking using these criteria could match optimization results when there is a significant difference in their values between candidates. According to the results of Table 2, methyl salicylate appears to be the best candidate due to both high driving forces and low $(E/D)_m$ and R_m, while 2-ethoxy ethanol looks worst. In between, MIBK exhibits the lowest $(E/D)_m$ but a larger R_m and the lowest driving forces. Compared to MIBK, phenol and ethyl benzoate show high driving forces but also less favourable (higher) $(E/D)_m$ and a slightly lower R_m for phenol, but a much higher R_m for ethyl benzoate. Hence, one must compare this preliminary ranking with the results of a more detailed simulation presented below.

3.4. Entrainer ranking based on optimization

In this section we discuss simulation results from the optimization procedure presented in section 2 and from Hu and Cheng's work (Hu and Cheng, 2017). For the same list of entrainers, these authors proposed a ranking on the TAC basis that confirms our combined ISS + driving force preliminary ranking. We found some inconsistencies in their results that prompted us to perform our own optimal simulation, which we present later.

First, compared to our simulation, Hu and Cheng's main feed enters the column at 25°C (instead of 54°C), which would impact mostly the reboiler heat duty in the extractive column. Second, they used a 6-mmHg pressure drop. This is not our case neither because we compare to the ISS method that uses constant pressure VLE diagrams (1 bar in our work). Note that there is no consensus in the literature as to whether lowering or increasing the pressure is beneficial to the process, as it may push the volatility either up or down, which can be detected by analysing the univolatility curves (Gerbaud et al., 2019). For the methanol - DMC extractive distillation with MIBK, Varyemez and Kaymak (2022) showed that increasing the operating pressure from 1 bar to 10 bar in the extractive column shifted the univolatility line closer to the product vertex and allowed reduction by 42.1% and 34.1% of the total reboiler heat duties and TAC, respectively, thanks to lower entrainer feed flowrate and reflux ratio. Thirdly, Hu and Cheng (2017) proposed for 2-ethoxy ethanol an optimal (E/D) lower than ISS $(E/D)_m$ value given in Table 2, which is not consistent. Comparison with ISS value is fair since, the ISS assumption of pure distillate matches the simulation high purity requirements, and Petlyuk's ISS method (Petlyuk et al., 2015) as well as other pinch methods (Knapp and Doherty, 1994, Brüggemann and Marquardt,

2004) have been proved to provide accurate estimations of minimal reflux and entrainer flow rate. After checking by simulation with Hu and Cheng parameters and (E/D) lower than ISS $(E/D)_m$ value, we indeed find that their published design cannot reach the expected purity as it enables to distillate merely 97.93 mol% methanol and 87.9 mol% DMC, which is well below their requirement claims. For this reason, we performed our own simulation results presented below.

Table 3 displays the results of the closed loop optimization study for methyl salicylate, phenol, MIBK, ethyl benzoate, 2-ethoxy ethanol carried out in this work. It provides information about tray numbers, feed locations, entrainer feed flow rate, reflux ratio, energy requirements, and costs. Simulations are based on feed conditions, yield recoveries and purity requirements listed in Table 1. The Q_c energy demand quantity adds the condenser heat removal at the column top and the heat removal for cooling the recycled entrainer stream. No heat integration is performed. Figure 6 displays the liquid composition profiles in the extractive distillation and the entrainer regeneration columns for each entrainer.

Table 3. Operating conditions for the extractive distillation column (C1) and the solvent regeneration column (C2)

	methyl salicylate		phenol		MIBK		ethyl benzoate		2-ethoxy ethanol	
	C1	C2	C1	C2	C1	C2	C1	C2	C1	C2
N $_{total}$	68	30	78	32	107	47	101	18	200	30
N $_{rectifying}$	4	16	4	15	48	21	5	7	5	12
N $_{extractive}$	55	-	61	-	51	-	81	-	165	-
N $_{stripping}$	9	14	13	17	8	26	11	11	30	18
E/D	1.09	-	1.61	-	0.89	-	2.45	-	6.19	-
E/F	0.93	-	1.37	-	0.76	-	2.09	-	5.28	-
E/E_m	1.17	-	1.47	-	1.31	-	1.27	-	1.24	-
Reflux ratio	0.30	0.60	0.64	2.20	2.10	6.50	0.89	1.18	6.00	20.00
Q_c (k)	-1853.3	-387.4	-2338,0	-773.9	-4419.4	-1762.6	-2694.3	-522.7	-9979.5	-4938.5
Q_r (k)	3095.7 [b]	1112.5 [a]	3903.3 [b]	1039.5 [a]	4933.4 [c]	1805.6 [c]	5557.4 [a]	1387.0 [a]	14419.3 [c]	5057.9 [c]
OPEX *(k$/year)*	*1119.3*		*1301.6*		*1605.5*		*2097.6*		*4642.0*	
CAPEX *(k$/year)*	*1276.6*		*1481.5*		*1923.3*		*1669.0*		*3911.0*	
TAC (k$/year)	1544.8		1795.5 (+16.2%)		2246.6 (+45%)		2654 (+72%)		5945.6 (+285%)	

[a] HP steam (41 barg, 527.15K) [b] MP steam (10 barg, 457.15K) [c] LP steam (5 barg, 433.15K)

methyl salicylate

Extractive column

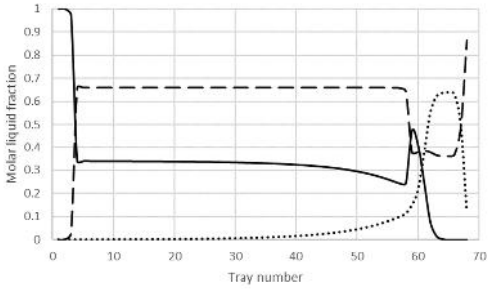

Solvent regeneration column

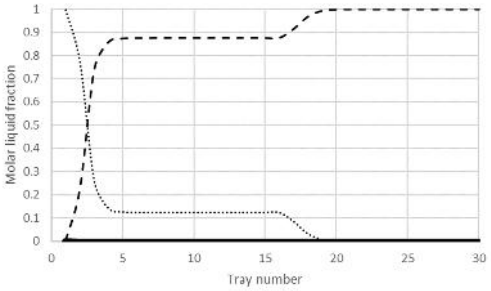

phenol

Extractive column

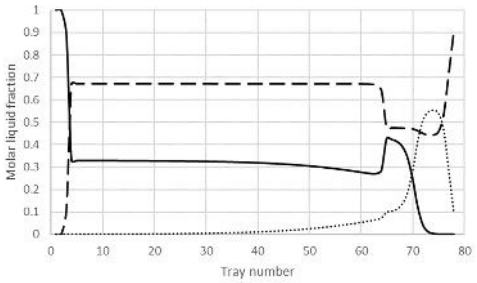

Solvent regeneration column

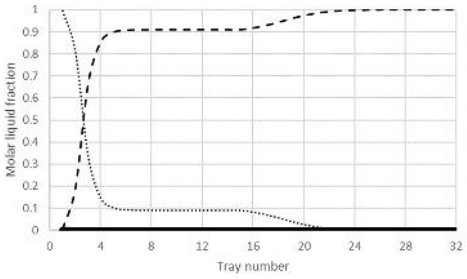

MIBK

Extractive column

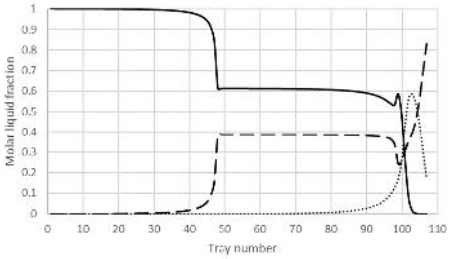

Solvent regeneration column

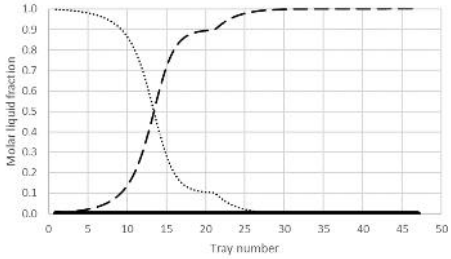

ethyl benzoate

Extractive column

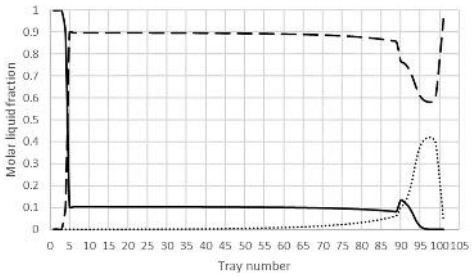

Solvent regeneration column

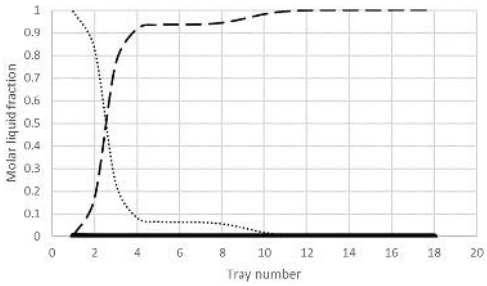

2-ethoxy ethanol

Extractive column

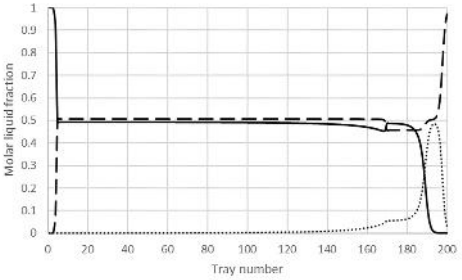

Solvent regeneration column

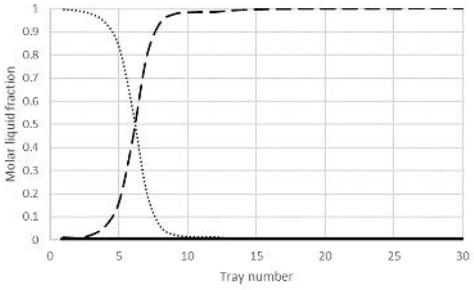

(—— methanol, ... DMC, — — entrainer)

Figure 6. Liquid profiles in extractive and solvent regeneration column

Regarding the results in Table 3, the first remark that the minimum TAC based ranking (without heat integration) agrees with the ranking obtained from coupling of the ISS method and driving forces concept that was discussed in section 3.3: ISS + driving force ranking sets methyl salicylate first, 2-ethoxy ethanol fifth and in between phenol (medium $(E/D)_m$ medium R_m and medium driving force), MIBK (lowest $(E/D)_m$ medium R_m but low driving force), and ethyl benzoate (higher $(E/D)_m$ much higher R_m but fairly good driving force). Figure 7 displays the trends of OPEX, CAPEX and TAC reported in Table 3 as well as the total heat duty for the reboilers. The highest boiler methyl salicylate allows the separation with the lowest CAPEX and OPEX because both columns have the lower trays number, reflux ratio and heat duty even if steam at middle and high pressure is required for the reboiler of the first and the second distillation column, respectively. Phenol is the second best entrainer because the extractive distillation requires more energy consumption and higher costs compared to methyl salicylate because of a higher entrainer flow rate and reflux ratio in both columns for similar number of trays. From the results in Table 2, phenol has higher values of $(E/D)_m$, R_m and lower driving forces than methyl salicylate. Although the MIBK entrainer flow rate is almost two times lower than for phenol, higher distillation columns and reflux ratios are needed leading to increase the OPEX, CAPEX and TAC. Varyemez and Kaymak (2022), who studied the extractive distillation of DMC-methanol with MIBK at 1 bar and from which we took the cost evaluation method, proposed another design with TAC within 2% of our design for MIBK. Differences arise for the extractive distillation with a shorter column due to a shorter extractive section (28 trays vs 51 for us). This would lower C_1 capital costs but higher operating costs as the entrainer flow rate (200 vs 128 kmol/h for our case) and reflux in C2 (7.38 vs 6.50). Interestingly, the CAPEX of ethyl benzoate is lower than that of MIBK with a similar total reboiler heat value even though the entrainer flow rate is more than double: driving forces of the ethyl benzoate are much higher, allowing separation with lower reflux ratios and fewer equilibrium trays mainly for the solvent recovery column (30 trays less than MIBK's C_2). Greater OPEX is caused by the higher ethyl benzoate flow rate and boiling temperature. The same reasoning about high boiling temperature holds for methyl salicylate: steam at medium and high pressure should be used in the first and second column, respectively.

Finally, 2-ethoxy ethanol is the worst entrainer by a large margin in both TAC and energy demand. This is due to high optimal (E/D) and R values (Table 3), which agree with the ISS values (Table 2). They boost the operating costs. Besides, low driving forces for 2-ethoxy ethanol manifest as a very large number of trays, increasing the capital costs. In Figure 7, one can observe that the short-cut entrainer ranking in *x*-axis, based on the values $(E/D)_m$, R_m and driving forces, is corroborated by the minimum TAC optimal simulations. The agreement

is clear when the values of the short-cut criteria are widely separated from each other (methyl salicylate vs ethoxy-ethanol) but less evident for the other candidates.

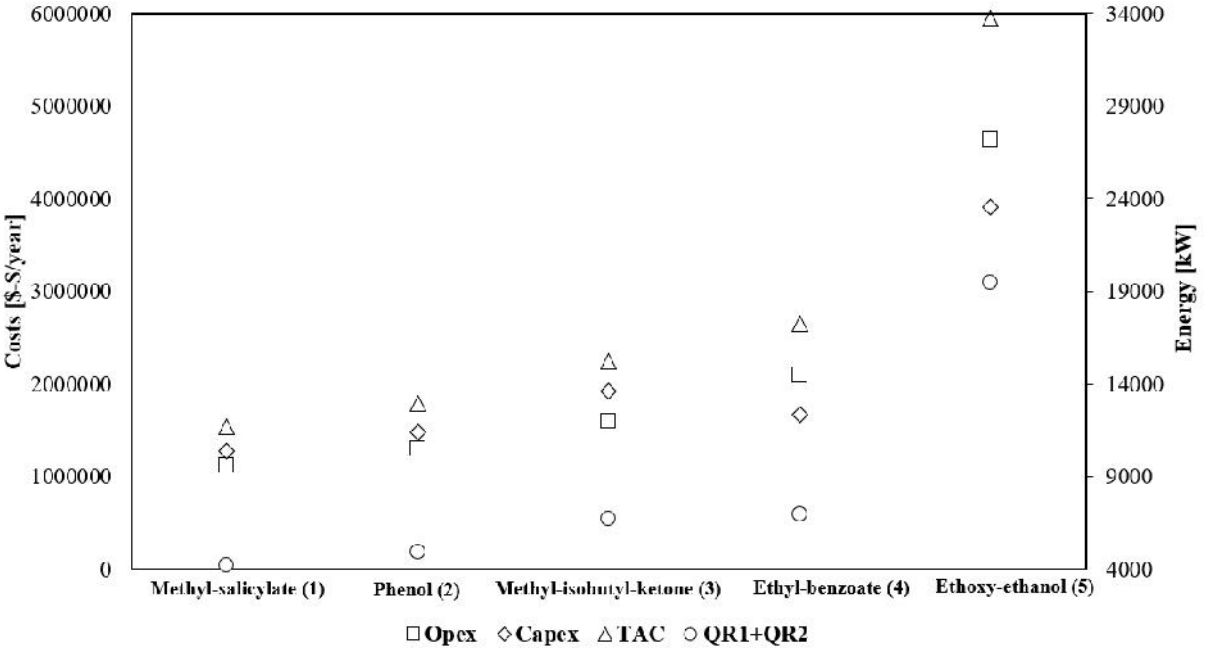

Figure 7. Costs and total heat duty vs short-cut method entrainer ranking

Another overall comment is that all optimal (E/D) values are higher than $(E/D)_m$ computed by ISS approach (Figure 7), in agreement with the feasibility conditions for extractive distillation (Knapp and Doherty, 1994, Brüggemann and Marquardt, 2004, Gerbaud et al., 2019). On the other hand, there is no well-established trend for R vs R_m . This is a known fact in extractive distillation column that when $(E/D) \geq (E/D)_m$, the corresponding operating R is not necessarily higher than R_m (Knapp and Doherty, 1994).

The third comment concerns the size of the columns, especially in the extractive section of C_1. As seen from the composition profiles shown in Figure 6, the number of trays is very large for all entrainers, and likely unrealistic for industrial implementation. This happens in this work as a result of the optimization procedure based on very high purity requirements for the methanol purity in the distillate. While being cautious to keep a process feasible within products requirements, removing some trays in distillation in general implies increased reflux ratios, leading to high reboiler duties, thereby shifting the balance between capital and operating costs. Notice that our cost evaluation is based on a standard method that should be adapted for specific conditions for the industrial use. Setting strict purity requirements and recovery yields, as we did, is also a cause of large columns needed so that composition profiles meet them. For example, as hinted by feasibility criteria for extractive distillation of the (1.0-1a) type extractive separation class (Gerbaud et al., 2019) in which A is a saddle in the residue curve map, high purity A (here ≥ 0.9999) is achieved only at the expense of barely no B component on the

entrainer feed tray which tops the extractive section. Figure 6 shows that this results in many trays in the extractive section so as to exhaust B and be able to connect the extractive section profile with a rectifying section profiles that can reach A purity location.

The fourth comment is that the optimal entrainer flow rate retrieved for each entrainer lies within the narrow range 1.2 – 1.5 times E_m as it is shown in Table 3. For comparison, Brüggemann and Marquardt (2004) proposed heuristics $E/E_m = 1.1$ and $R_m /R_m = 2.0$ while Knapp and Doherty (1994) prescribed to use the classical value $R_o /R_m \in [1.2 - 1.5]$ and found empirically that $E/E_m \in [2.0 - 4.0]$ corresponded to a design within "10-15% of the lowest cost design".

In general, shorter distillation columns are related to high driving force values. On one hand, high values of D_A^A enhance the separation of azeotropic compounds into the rectifying and extractive section of the extractive distillation column. Besides, high values of D_B^B are also needed to minimize the cost and the energy consumption of the second distillation column. On the other hand, similar values of D_A^A and D_B^B may decrease the separation efficiency of the extractive section. Furthermore, Cignitti et al. (2019) suggested that an optimal value of the ratio D_A^A /D_B^B (circa 1.2 for their acetone – methanol separation case study) would lower both TAC and energy demand. However, looking at the results in Table 2, the picture is less clear. The lowest TAC and energy demand entrainer, methyl salicylate, agrees with Cignitti's prescription with a ratio D_A^A /D_B^B of 1.14. But ethyl benzoate has also a ratio D_A^A /D_B^B 1.18, display high driving forces like methyl salicylate but is ranked fourth. Both entrainers have similar tray numbers in the rectifying and the stripping section but for methyl salicylate the extractive section number of trays is half of that calculated for ethyl benzoate. These results indicate that for the C1 column, the ratio of D_A^A /D_B^B should not be examined alone, but together with the other two criteria $(E/D)_m$ and R_m from the ISS method, as we propose in this work. Regarding each column composition profile in the driving force map (Figure 7), the driving force $(y_A - x_A)$ inside the extractive column is mainly located in the region where driving force D_A^A is large. This is caused by the primary goal of the first extractive column that aims at distillation of methanol (A). For the regeneration column, it behaves as pseudo-binary distillation column splitting B and E. One can also notice that low D_B^B implies a large column, like for MIKB. Gani and Pedersen (2000) further prescribed to set the feed inlet in the large D_B^B region. In our case, this happens only for methyl salicylate and not for the other entrainers (Figure 7). So, TAC optimization is not agreeing with that heuristic in our case, possibly because the entrainer regeneration feed inlet.

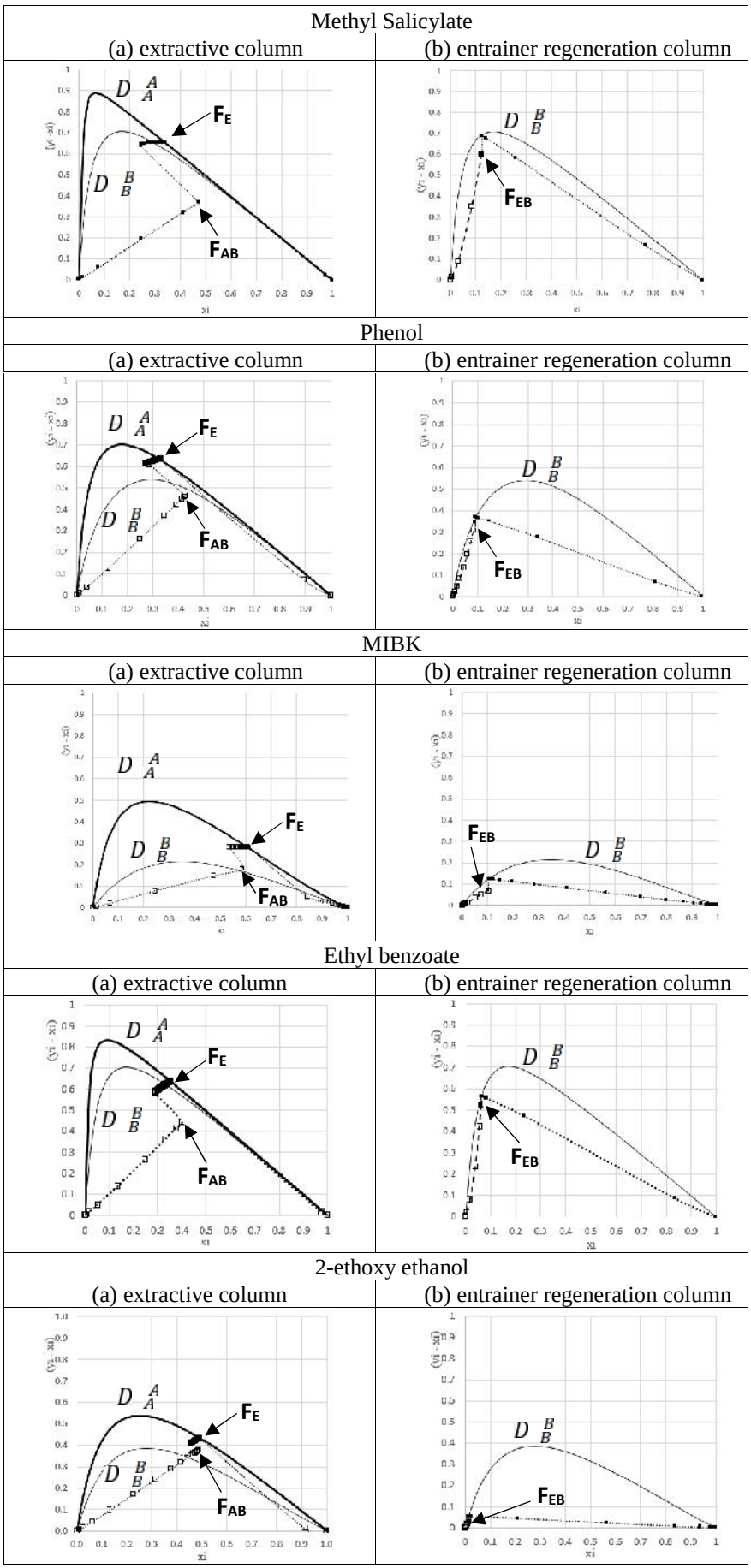

Figure 7. Optimal liquid profile into the extractive column and the entrainer recovery column along with driving force curves D_A^A and D_B^B with i: methanol or DMC, respectively

4. Conclusions

Entrainer selection is a crucial step in process synthesis and design of extractive distillation processes. Over the years, simple criteria have shown their limitations when compared to optimal simulation results, like criteria based on thermodynamic calculations into the infinite dilution entrainer domain. A new methodology has been proposed in this paper coupling the infinite sharp splits (ISS) method with other thermodynamic criteria related to driving forces concept. Calculation of all criteria only needs a model of the vapour – liquid equilibrium for each involved binary mixture and the vapour pressure of pure compounds. The ISS method allows the calculation of the limiting values of the entrainer flow rate $(E/D)_m$ and the reflux ratio R_m of the extractive column while the driving force concepts are related to the conventional separation in the solvent recovery. For the extractive distillation process of the minimum-boiling azeotropic mixture methanol – DMC with five entrainers, the ranking proposed by the combined short cut calculations are compared by the simulated design ranking resulting from TAC optimization. In general, an entrainer having low $(E/D)_m$ and R_m as well as high driving forces would allow the separation by extractive distillation process involving shorter columns with small entrainer flow rate and reflux ratio. That is the case when entrainers being compared having very large differences between all criteria and they follow the appropriate trend. In fine, the short-cut ranking and the optimization ranking agree that methyl salicylate is ranked first and 2-ethoxy ethanol is last, with entrainer flow rate, reflux and driving force being the most favourable for methyl salicylate and by far the worst for 2-ethoxy-ethanol. When the criteria values $(E/D)_m$, R_m , $D\ {}^{A}_{A}$ and $D\ {}^{B}_{B}$ are closer, the observed agreement between both ranking is more difficult to explain and seems related to specific characteristics of the entrainers and their impact on the CAPEX and OPEX of the extractive process. That happens when comparing MIBK with phenol and ethyl benzoate. Phenol ranks second in the optimized TAC results, even if $(E/D)_m$ for MIBK (ranked third) is almost the half of phenol and three times lower than that of ethyl benzoate (ranked fourth). The MIBK process requires higher columns and substantial reflux ratios due to the much lower driving forces, even when compared to the ethyl benzoate process. CAPEX and OPEX. Despite similar total heat duty for ethyl benzoate and MIBK, ethyl benzoate displays a lower CAPEX, explained by greater driving forces of ethyl benzoate; similar to those of first-ranking methyl salicylate; enabling the separation with shorter distillation columns and low reflux ratio than MIBK. However, the OPEX is greater for ethyl benzoate because the 2.5 time higher of the entrainer flow rate and the most significant boiling point imposing the use of middle and high steam pressure. The impact of the price and the boiling point of the entrainer in the OPEX is controversial because it depends on the optimal entrainer flowrate. For the two connected

columns working in a closed loop process that we consider, there is no clear weighting of the individual criteria. These results demonstrated that a multiplex relationship exists between $(E/D)_m$, R_m and driving forces D_A^A and DF_B^B even for the extractive distillation column alone.

In detail for the case studied, our results rule out the common selectivity criteria for screening entrainer and they show that the information provided by the location of the univolatility curve related to $(E/D)_m$ is more relevant. Besides, we confirm that the higher the maximum value of the driving force of the high boiling azeotropic compound with the entrainer, the less energy and number of equilibrium trays is required for the entrainer recovery column. As prescribed by Cignitti et al., (2019), the entrainer with the lowest TAC and energy demand, methyl salicylate shows a ratio D_A^A / D_B^B near 1.2, but one notice that this ratio alone is not decisive, as the fourth ranking entrainer, ethyl benzoate, has similar driving forces. Instead, ratio D_A^A / D_B^B should be examined together with the other two criteria $(E/D)_m$ and R_m computed from the ISS method.

The combined ISS method – driving force criteria studied in this work rely upon readily available thermodynamic data and need a limited computation effort, compared to optimization based on process simulation. In our case study, it also agrees more closely with entrainer ranking from optimization studies than the classic criteria based on infinite dilution selectivity. If tested on other case studies, the proposed methodology might allow a rapid identification of the suitable candidates to be investigated further. Hence, they can contribute to develop a suitable set of requirements enabling the computer-aided molecular design of potential entrainer candidates based on integrated process/product design approach.

Declarations

The authors declare that they have no known competing financial interests or personal relationships that could have appeared to influence the work reported in this paper.

They also used no generative AI nor any AI-assisted tools to produce the content of this paper.

References

Brüggemann, S., Marquardt, W., 2004. Shortcut methods for nonideal multicomponent distillation: 3. Extractive distillation columns. AIChE J. 50, 1129–1149.

Cignitti S., Rodriguez-Donis I., Abildskov J., You X., Shcherbakova N., Gerbaud V., 2018. CAMD for Entrainer Screening of Extractive Distillation Process Based on New Thermodynamic Criteria. Chem. Eng. Trans., 69, 223-228.

Cignitti, S., Rodriguez-Donis, I., Abildskov, J., You, X., Shcherbakova, N., Gerbaud, V., 2019, CAMD for entrainer screening of extractive distillation process based on new thermodynamic criteria, Chem. Engin. Res. Des., 147, 721–733.

Cots O., Shcherbakova N., Gergaud J., 2021. SMITH: differential homotopy and automatic differentiation for computing thermodynamic diagrams of complex mixtures. Computer Aided Chem. Eng., 50,1081-1086.

Gani, R., Bek-Pedersen, E., 2000. Simple new algorithm for distillation column design. AIChE J. 46, 1271–1274.

De Figueirêdo, M.F., Guedes B.P., de Araújo, J.M.M., Vasconcelos, L.G.S., Brito, R.P., 2011. Optimal design of extractive distillation columns—A systematic procedure using a process Simulator. Chem. Eng. Res. Des. 89, 341–346.

García-Herreros P., Gómez, J.M., Gil, I.D., Rodríguez, G., 2011.Optimization of the Design and Operation of an Extractive Distillation System for the Production of Fuel Grade Ethanol Using Glycerol as Entrainer. Ind. Eng. Chem. Res. 50(7), 3977-3985.

Gerbaud, V., Rodriguez-Donis, I., Lang, P., Denes, F., Hegely, L., You, X., 2019. Review of Extractive Distillation: process design, operation optimization and control. Chem. Eng. Res. Des., 141, 229-271.

Gu, J, You, X.Q., Tao, C., Li, J., Gerbaud, V., 2018. Energy-saving reduced pressure extractive distillation with heat integration for separating biazeotropic ternary mixture tetrahydrofuran-methanol-water. Ind. Eng. Chem. Res., 57 (40), 13498-13510.

Hilmen, E.K., Kiva, V.N., Skogestad, S., 2002. Topology of Ternary VLE Diagrams: Elementary Cells. AIChE J. 48(4), 752–759.

Hsu, K.H., Hsiao, Y.C., Chien, I.L., 2010. Design and Control of Dimethyl Carbonate−Methanol Separation via Extractive Distillation in the Dimethyl Carbonate Reactive-Distillation Process. Ind. Eng. Chem. Res., 49, 2, 735–749.

Huang, H., Samsun, R.C., Peters, R., Stolten, D., 2021. Greener production of dimethyl carbonate by the Power-to-Fuel concept: a comparative techno-economic analysis. Green Chem. 141, 229-271.

Hu, C.C., Cheng, S.H., 2017. Development of alternative methanol/dimethyl carbonate separation systems by extractive distillation - A holistic approach. Chem. Eng. Res. Des., 127, 189-214.

Kiva, V.N., Hilmen, E.K., Skogestad, S., 2003. Azeotropic Phase Equilibrium Diagrams: A Survey. Chem. Eng. Sci. 58, 1903-1953.

Knapp, J.P., Doherty, M.F., 1994. Minimum entrainer flows for extractive distillation: A bifurcation theoretic approach. AIChE J. 40, 243-268.

Kossack, S; Kraemer, K., Gani, R., Marquardt, W., 2008. A Systematic Synthesis Framework for Extractive Distillation Processes. Chem. Eng. Res. Des. 86, 781-792.

Laroche, L., Bekiaris, N., Andersen, H.W., Morari, M., 1991. Homogeneous azeotropic distillation: comparing entrainers. Can. J. Chem. Eng. 69, 1302-1319.

Laroche, L., Bekiaris, N., Andersen, H.W., Morari, M., 1992a. Homogeneous azeotropic distillation: separation and flowsheet synthesis. Ind. Eng. Chem. Eng. 31, 2190-2209.

Laroche, L., Bekiaris, N., Andersen, H.W., Morari, M., 1992b. The curious behavior of homogeneous azeotropic distillation – implications for entrainer selection. AIChE J. 38, 1309-1328.

Lei, Z., Li, C., Chen, B., 2003. Extractive Distillation: A Review. Sep. Purif. Rev. 32(2), 121–213.

Lelkes, Z., Lang P., Benadda B., Moszkowicz P., 1998. Feasibility of extractive distillation in a batch rectifier, AIChE J. 44, 4, 810-822.

Levy, S.G., Van Dongen, D.B., Doherty, M.F., 1985. Design and synthesis of homogeneous azeotropic distillations. 2. Minimum reflux calculations for nonideal and azeotropic columns. Ind. Eng. Chem. Fundam. 24(4), 463-474.

Luyben, W.L., Chien, I. L., 2010. Design and Control of Distillation Systems for Separating Azeotropes. Wiley-VCH, New York, 453 p.

Matsuda, H., Negishi, M., Iino, S., Constantinescu, D., Kurihara, K., Tochigi, K., Ochi, K., Gmehling, J., 2019. Isothermal vapor–liquid equilibria at 383.15–413.15 K for the binary system methanol + dimethyl carbonate and the pressure dependency of the azeotropic point. Fluid Phase Equilibria 492, 101–109.

Mathematica®. http://www.wolfram.com/mathematica/

Momoh, S.O., 1991. Assessing the accuracy of selectivity as a basis for solvent screening in extractive distillation processes. Sep Sci Technol, 26(5), 729–742.

Petlyuk, F.B., Danilov, R.Yu., 1999. Sharp Distillation of Azeotropic Mixtures in a Two-Feed Column. Theor. Found. Chem. Eng. 33, 233–242.

Petlyuk, F. B., 2004. Distillation Theory and Its Application to Optimal Design of Separation Units. Cambridge Series in Chemical Engineering. Cambridge University Press, Cambridge, UK. 362 p.

Petlyuk, F., Danilov, R., Burger, J., 2015. A novel method for the search and identification of feasible splits pf extractive distillations in ternary mixtures, Chem. Eng. Res. Des. 99, 132-148.

Petlyuk, F., Danilov, R., Adiche, C., 2021. Using the Method of Infinitely Sharp Splits for the Optimal Design of Extractive Distillation Units. 1. Ternary Mixtures, Ind. Eng. Chem. Res. 2021, 60, 16430−16444.

Pretel, E.J., López, P.A., Bottini, S.B., Brignole, E.A., 1994. Computer-aided molecular design of solvents for separation processes. AIChE J. 40(8) 1349-1360.

Seihoub, F.Z. PhD thesis. 2018. Design et développement des procédés de séparation des mélanges idéaux et non idéaux dans des colonnes de distillation et distillation extractive à cloison. Université des Sciences et de la Technologie d'Oran Mohamed Boudiaf. Algerie.

Shcherbakova, N., Rodriguez-Donis, I., Abidskov, J., Gerbaud V., 2017a. A Novel Method for Detecting and Computing Univolatility Curves in Ternary Mixtures. Chem. Eng. Sci., 173, 21-36.

Shcherbakova N., Rodriguez – Donis I., Abildskov J., Gerbaud V., 2017b. Univolatility curves in ternary mixtures: geometry and numerical computation. Computer Aided Chem. Eng., 40, 229-234.

Shcherbakova N., Rodriguez-Donis I., Abildskov J., Gerbaud V., 2018. Univolatility curves in ternary mixtures: topology and bifurcation. Chem. Eng. Trans., 69, 73-78.

Shen, W., Benyounes, H., Gerbaud, V., 2013. Extension of Thermodynamic Insights on Batch Extractive Distillation to Continuous Operation. 1. Azeotropic Mixtures with a Heavy Entrainer. Ind. Eng. Chem. Res. 52(12), 4606–4622.

Skiborowski, M., Rautenberg, M., Marquardt, W. 2015. A Hybrid evolutionary-deterministic optimization approach for conceptual design. Ind. Eng. Chem. Res. 51 (41), 10054-10072.

Varyemez, H.S. Kaymak, D. B., 2022. Effect of operating pressure on design of extractive distillation process separating DMC-MeOH azeotropic mixture. Chem. Eng. Res. Des., 177, 108-116.

Yang, A., Sun, S., Shi, T., Xu, D., Ren, J., Shen, W., 2019. Energy-efficient extractive pressure-swing distillation for separating binary minimum azeotropic mixture dimethyl carbonate and ethanol. Sep. Pur. Tech. 229, 11587 - 11598.

You, X., Rodriguez-Donis, I., Gerbaud, V. 2014. Extractive distillation process optimisation of the 1.0-1a class system, acetone - methanol with water. Comput. Aided Chem. Eng. 33, 1315-1320.

You, X., Rodriguez-Donis, I., Gerbaud, V., 2015. Investigation of Separation Efficiency Indicator for the Optimization of the Acetone-Methanol Extractive Distillation with Water. Ind. Eng. Chem. Res. 54 (43), 10863-10875.

You, X., Rodriguez-Donis, I., Gerbaud, V., 2016. Low pressure design for reducing energy cost of extractive distillation for separating diisopropyl ether and isopropyl alcohol. Chem. Eng. Res. Des., 109, 540-552.